

A weakly coupled implementation of hydrogen embrittlement in FE analysis

Giorgia Gobbi¹, Chiara Colombo, Stefano Miccoli, Laura Vergani

Politecnico di Milano, Department of Mechanical Engineering,
Via G. La Masa 1, 20156 Milano, Italy


Manuscript Info

[October 1, 2018] This is an author generated postprint of the article:

“G. Gobbi, C. Colombo, S. Miccoli, L. Vergani, A weakly coupled implementation of hydrogen embrittlement in FE analysis, *Finite Elements in Analysis and Design*, Volume 141, 2018, Pages 17–25, ISSN 0168-874X, doi 10.1016/j.finel.2017.11.010.”

The version of record is available at <https://doi.org/10.1016/j.finel.2017.11.010>

The software described in this paper is available at <https://doi.org/10.5281/zenodo.1442399>

©2018. This manuscript version is made available under the Creative Commons Attribution-NonCommercial-NoDerivatives 4.0 International License. 

Abstract

The paper presents a numerical code for the simulation of hydrogen embrittlement. The aim is to provide a guideline to the methodology but also to its practical use. The code, implemented within the commercial software Abaqus, presents a three-step procedure that weakly couples hydrogen diffusion with stress–strain analysis:

1. an initial static analysis,
2. a mass diffusion analysis, and
3. a final static analysis with the cohesive zone modelling approach.

Cohesive elements offer a customizable formulation within the standard finite element framework, and are suitable to simulate failure of the material (i. e. a crack) in presence of environmental hydrogen uptake. The formulation of cohesive elements is implemented considering a mechanism of local decohesion with an extensive use of Abaqus user subroutines. Examples of the code application to simple models and to a real specimen are included to support as well as to make the findings of the paper fully replicable. All the subroutines and the examples are released in open source form under the webpage of the project, named PoliHydra.

Keywords: Hydrogen embrittlement, Finite element method, Cohesive elements

1. Introduction

Hydrogen embrittlement phenomenon is responsible for several failures of components or structures that most of the time lead to dangerous consequences for environment, industrial economy and personnel health. Hydrogen embrittlement was extensively investigated from the experimental and analytic standpoint [1–3]. However, there is still a controversial point: the definition of a univocal micromechanism to describe the hydrogen embrittlement. Until now, three main mechanisms were

proposed: Hydrogen-Enhanced DEcohesion (HEDE) [1], Hydrogen Enhanced Localized Plasticity (HELP) [4] and hydride formation and cleavage [5]. Despite this open issue, in order to design efficient components during their service life, it is essential to have also numerical tools able to predict the mechanical response of the material to extreme environmental conditions. To this end, recently, predictive finite element (FE) models for estimating the mechanical behaviour of steels in presence of hydrogen were developed. These models include both hydrogen diffusion and stress–strain analysis during crack propagation, simulated by using cohesive technique. The cohesive law accounts for the presence of hydrogen in the material surrounding

¹Currently CERN, EN Department, MME-EDS Group, Geneva Switzerland.

the crack tip thus reproducing the embrittlement phenomenon. In the literature, with reference to the commercial FE software Abaqus, two approaches were proposed to solve this problem.

The first approach suggested by Olden *et al.* [6, 7] partially decouples hydrogen diffusion process from stress–strain analysis through a three-step procedure:

1. first a static analysis is performed to evaluate the hydrostatic stress state;
2. second a mass diffusion analysis determines the diffusible hydrogen content, C_L ;
3. finally a “cohesive stress” analysis is performed to calculate the trapped hydrogen amount, C_T , the total hydrogen concentration, C , and to simulate the crack initiation/propagation in the steel.

This procedure was applied to 2D and 3D models [8, 9] to predict the crack initiation for a material containing hydrogen.

The second approach instead fully couples hydrogen diffusion and stress–strain analysis during crack propagation in a single simulation. Brocks *et al.* [10] employed the coupled model to investigate the effect of the deformation rate on the hydrogen embrittlement process of a low alloy steel, FeE 690T. Recently, Moriconi *et al.* [11] applied the same model extending the application to cyclic loads on a martensitic stainless steel, 15P-5.

Both the above mentioned approaches are not possible within the “core” Abaqus software, but require writing custom “*user subroutines*”, which however are not readily available. Therefore, the authors developed a new implementation for both the two approaches, code-named HYDRA, released in open source form. HYDRA was developed to simulate the fracture toughness test of a C(T) specimen made of a high-strength steel, AISI 4130 (UNS G41300), charged with atomic hydrogen. Hence, the current version allows for solving 2D plain strain problems for both small and large displacement formulations, considering reduced integration elements. Due to the problem symmetries, only mode I loading was considered, and the in-plane sliding mode was not taken into account. These limitations will be removed in a future release and are the object of an ongoing research project.

The aim of the current paper is to provide a guideline to the methodology but also to the practical use of the above mentioned open source Abaqus code, focusing herein only on the three-step procedure. A companion paper will illustrate the fully coupled procedure. The full code and more detailed instructions and examples are provided in [12].

The paper is organized as follows. First, an outline of the adopted cohesive model is proposed, by defining the corresponding Traction–Separation Law (TSL) and briefly outlining its calibration with reference to a given material, without taking into account the presence of hydrogen. Then, the three-step analysis to simulate the effect of hydrogen on the material mechanical properties is illustrated.

List of symbols

A	current value of the continuum element cross area, normal to the load application
A_0	initial value of the continuum element cross area, normal to the load application
C	total hydrogen content
C_L	diffusible content of hydrogen
C_T	trapped content of hydrogen
\mathcal{D}	material damage
D_L	diffusivity of hydrogen in lattice sites
E_{nn}	stiffness of the cohesive element along direction n
J	hydrogen flux
k	factor decreasing cohesive strength, based on HEDE mechanism
k_p	pressure stress factor
L	current value of the continuum element length
L_0	initial value of the continuum element length
n, s	normal (mode I) and shear (mode II) directions
p	equivalent pressure stress (hydrostatic stress)
R	universal gas constant
s	solubility of the as-received material
T	absolute temperature
t	nominal traction stress
t_n^*	corrected nominal traction based on the current cross area A
t_n^0	limit stress of the cohesive element
$t_{n,elastic}$	normal elastic stress
T_0	initial constitutive thickness of the cohesive element
u	displacement along y axis
\bar{V}_H	molar volume fraction of hydrogen in iron
x, y	main reference frame
δ	relative displacement between the cohesive element faces
δ_0	displacement at the end of the elastic behaviour of the cohesive element
δ_1	displacement at the end of the softening behaviour of the cohesive element
δ_F	displacement at the final failure of the cohesive element
δ_n	normal relative displacement between the cohesive element faces
Δg_b	variation of Gibbs free energy
ϵ_n	nominal strain
ϵ_n^0	limit strain of the cohesive element
ϵ_p	plastic strain
θ	hydrogen coverage factor
σ	Cauchy stress of the continuum element

ϕ	normalized concentration
<i>List of acronyms</i>	
C(T)	compact tension specimen
CTOD	crack tip opening displacement
HEDE	Hydrogen Enhanced DE-cohesion, embrittling mechanism
IP	integration point
LE	logarithmic deformation of the continuum element
MPC	multi-point constraint
TSL	Traction–Separation Law

2. Traction–Separation Law

The cohesive elements are particular finite elements implemented to describe the interface mechanical behaviour. Initially introduced to simulate interfacial debonding of adhesives, later on they have been extended to fracture mechanics issues. For such purpose, the crack-processing region is discretized with a layer of cohesive elements whose constitutive behaviour is not related to the global properties of the material. On the contrary, the constitutive law of the cohesive elements is described by local forces acting at the crack surface and tip, expressed as Traction–Separation Law $t-\delta$ (Fig. 1). t is the nominal traction stress, which has the dimensions of a force per unit area [FL⁻²] and δ is the relative displacement between the cohesive element faces, which has the dimensions of a length [L]. Typically, t and δ are vector quantities whose components are defined in an element-local reference frame, $n-s$, where n is the normal (mode I) direction and s is the in-plane local shear (mode II) direction [13]. As mentioned before, for symmetry reason of the considered problem for which the code was developed, the shear component t_s vanishes. Accordingly, below a simplified account of the Traction–Separation Law will be given, considering only the normal components n .

The TSL model available in the Abaqus library assumes an initial linear elastic behaviour followed by initiation and evolution of damage. In regard to the initial linear elastic part, the Traction–Separation Law is expressed as

$$t_{n,\text{elastic}} = E_{mn} \frac{\delta_n}{T_0} \quad (1)$$

where T_0 is the *initial constitutive thickness*. T_0 does not have a physical meaning, but is only a normalization factor that allows to define a *nominal* strain

$$\epsilon_n = \frac{\delta_n}{T_0}$$

such that the terms in $t_{n,\text{elastic}} = E_{mn} \epsilon_n$, have the same dimensions as in the case of a classical continuum mechanics stress–strain curve. Typically, T_0 is set equal to 1 unit-of-length, so that δ_n and ϵ_n have the same numerical value, although different dimensions.

In regard to progressive damage modelling, it is composed by two parts, damage initiation, and damage evolution. For the case in which only the normal component exists, damage initiation can be expressed equivalently as a maximum stress or maximum strain criteria

$$\frac{\langle t_n \rangle}{t_n^0} = 1, \quad \frac{\langle \epsilon_n \rangle}{\epsilon_n^0} = 1$$

where the Macaulay bracket $\langle \cdot \rangle = \max\{0, \cdot\}$ expresses the fact that normal compressive stresses or strains do not induce damage; t_n^0 and ϵ_n^0 are the limit stress and strain respectively. However, in case of nonlinear geometric effects, the maximum strain criterion is preferred. Indeed, in Abaqus traction across the cohesive element is always defined as a nominal one (nodal force over initial cross area); therefore, for significant changes in the element cross area, quantity t_n loses its physical meaning. This point is further analyzed below, see eqs. (4)–(5).

When the selected damage initiation criterion is met, the material damage can be described as a function of a scalar variable, \mathfrak{D} , which represents the overall damage in the material related to all the active mechanisms. It initially has a value of 0 (no damage); when damage occurs, \mathfrak{D} monotonically evolves from 0 to 1. The normal stress component of the traction–separation model is affected by the damage according to

$$t_n = \begin{cases} (1 - \mathfrak{D}) t_{n,\text{elastic}} & t_{n,\text{elastic}} \geq 0 \\ t_{n,\text{elastic}} & \text{otherwise} \end{cases} \quad (2)$$

where $t_{n,\text{elastic}}$ is the stress component predicted by the elastic traction–separation behaviour for the current separation without damage. Typically the evolution of \mathfrak{D} is considered as a function of δ_n .

A TSL with a trapezoidal shape (Fig. 1) was chosen, because it can properly represent the elastic-plastic behaviour of steel [14]. The corresponding evolution of \mathfrak{D} , for monotonically increasing δ_n , is described by the following set of equations:

$$\mathfrak{D}(\delta_n) = \begin{cases} 0 & \text{for } \delta_n \leq \delta_0 \text{ (elastic)} \\ 1 - \frac{\delta_0}{\delta_n} & \text{for } \delta_0 < \delta_n \leq \delta_1 \text{ (plateau)} \\ 1 - \frac{\delta_0}{\delta_n} \left(\frac{\delta_F - \delta_n}{\delta_F - \delta_1} \right) & \text{for } \delta_1 < \delta_n \leq \delta_F \text{ (softening)} \\ 1 & \text{for } \delta_n > \delta_F \text{ (failure)} \end{cases} \quad (3)$$

For unloading, i.e. decreasing separation δ_n , the damage \mathfrak{D} is kept constant, effectively resulting in a degradation of the cohesive “stiffness” from E_{mn} to $\mathfrak{D}E_{mn}$.

When considering inter-element equilibrium between cohesive and solid elements, care must be taken to the spatial integration of the internal work term in the principle of virtual work. For solid elements, Abaqus defines two different integration strategies, with respect to the **NLGEOM** parameter.

- With **NLGEOM=NO** (the default) nonlinear geometric effects are neglected, and nodal forces are computed by integrating the principle of virtual work over the reference configuration; accordingly stresses are defined as nominal ones.

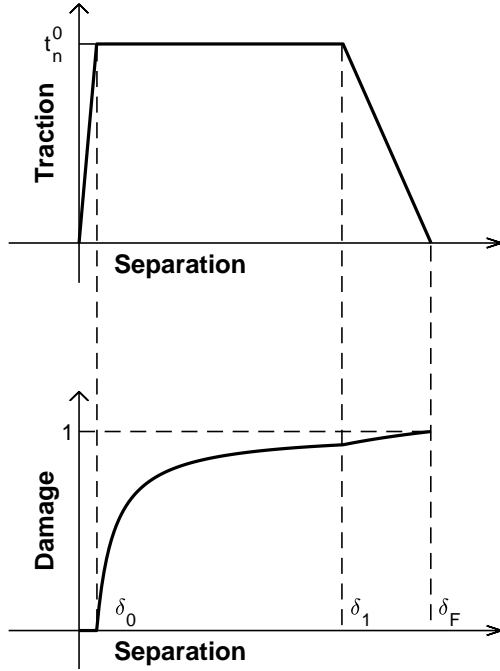


Figure 1: TSL and Damage curve.

- With `NLGEOM=YES`, the integration is performed with reference to the current configuration, and correspondingly stresses are defined as true, or Cauchy stresses.

Unfortunately, for cohesive elements, Abaqus integrates always over the reference configuration, i.e. over the initial area, so that traction t in the TSL is always defined as a nominal one. However, as pointed out in Ref. [14], in case of crack propagation in ductile materials, the area of the cohesive elements can change significantly due to plastic deformation. If the analysis is performed with `NLGEOM=ON`, this leads to significant discontinuities between the true stress values calculated in the solid elements and the traction t of the adjacent cohesive elements.

Therefore, it is necessary to correct the calculation considering the current area of the cohesive element. To this end, under the assumption of plain strain, the total logarithmic deformation `LE11` of each adjacent solid element can be used to compute the reduced area as follows:

$$\frac{A}{A_0} = \frac{L}{L_0} = \exp(\text{LE11}) \quad (4)$$

where A , L are the current values of area and length, A_0 and L_0 are the initial values, respectively and the analysis 11 direction has to be aligned to the cohesive shear direction s . To introduce the effect of area reduction in Abaqus, it is sufficient to define a corrected “nominal traction”

$$t_n^* = \frac{A}{A_0} t_n \quad (5)$$

so that $t_n^* \cdot A_0 = t_n \cdot A$, and the nodal equivalent forces computed using $t_n^* \cdot A_0$ (Abaqus) are equal to those computed using $t_n \cdot A$ (large displacement formulation). The corrected value t_n^* can be

introduced in Abaqus by changing the value of E_{nn} as a function of the adjacent solid element logarithmic strain:

$$E_{nn}^* = E_{nn} \exp(\text{LE11}) \quad (6)$$

This is obtained by specifying `DEPENDENCIES=1` on the cohesive `*ELASTIC` card and a `USDFLD` user subroutine.

2.1. Example

Herein, a very simple example is reported to illustrate how the code works.² The geometry is shown in Fig. 2. It consists of a 2D plane problem, made of a linear cohesive element, E1, associated with a bilinear quadrilateral continuum element with plane strain formulation, E2. The cohesive element corresponds to the location of a possible crack. Reduced integration was selected for the continuum element, meaning that field quantities are evaluated at the single Gauss point placed at its centre, while cohesive elements have two Gauss points (see Fig. 2). The choice of considering the reduced integration for continuum elements directly allows to calculate each field quantity as a unique value for each element, thus avoiding any further operation of extrapolation or averaging. The applied load is monotonic and uni-axial (mode I test). The simulation is run under displacement control, applying the same displacement \bar{u}_y to the two upper nodes of the continuum element. The material of the continuum element is a high-strength steel, AISI 4130, whose mechanical properties are defined into the `_AISI.inp` file according to [15]. The constitutive law of the cohesive element, instead, is defined in `_coh.inp` file. It is created automatically by means of a Python script, which includes the formula presented in Eq. 3. As damage initiation criterion, the maximum nominal strain (card `*DAMAGE INITIATION, CRITERION=MAXE`) was selected. Then, the card

`*DAMAGE EVOLUTION, TYPE=DISPLACEMENT, SOFTENING=TABULAR`

provides the values of \mathfrak{D} and δ_n that describe plateau and the failure parts of the TSL.

2.2. Results

Figure 3a represents the TSL of the cohesive element obtained by plotting the normal component of the stress, t_n , calculated in the cohesive element at integration point IP1 as a function of the displacement of the node 3 (solid line). In the same figure the correction of eq. (5) is applied for different values of `LE11`.

The effect of the true stress on the cohesive law is visible in Fig. 3b that reports the σ_{yy} stress component calculated on the continuum element (solid line) along with the cohesive element traction t_n^* (dashed line) as a function of the displacements of node 5. Two different TSL were tested with two t_0 values, 1000 MPa and 1200 MPa. The Cauchy stress σ_{yy} correctly tops at these values, while t_n^* has a lower value due to the fact that the $\epsilon_{11} > 0$ implies that the cohesive element current area A is greater than the initial one A_0 , eq. (5).

²The input files for this and the subsequent examples are available online [12] in the download/verification section.

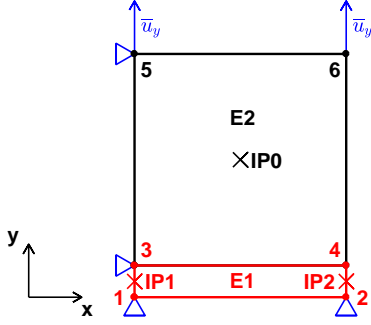
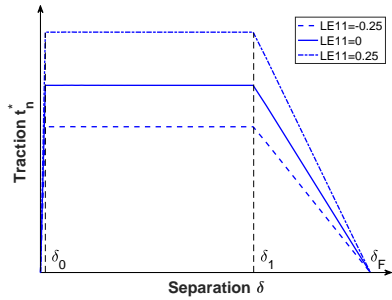
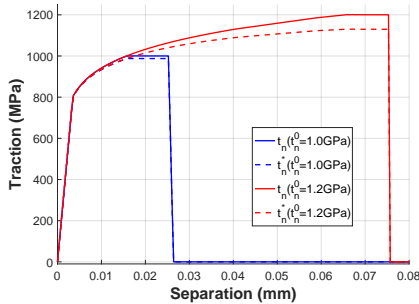


Figure 2: TSL verification model, single cohesive element E1 and single continuum element E2. Vertical displacements are constrained at nodes 1, 2 and horizontal displacements at nodes 3, 5. A vertical displacement \bar{u}_y is applied at nodes 5, 6. The integration points IP for both elements are shown.



(a)



(b)

Figure 3: (a) Corrected TSL t_n^* accounting for different values of LE11. (b) Corrected t_n^* at integration point IP1, and Cauchy stress σ_{yy} at integration point IP0, as a function of displacement \bar{u}_y at node 5.

3. Hydrogen embrittlement simulation

The code was developed to simulate the effect of hydrogen on a high-strength steel during a fracture toughness test. The model framework is the one proposed in Ref. [6] that progressively couples the stress-strain fields with hydrogen diffusion-trapping mechanisms by means of three steps of simulations.

Indeed, the diffusible content of hydrogen, C_L , that moves through the interstitial sites of the steel lattice and the content of hydrogen trapped by material inhomogeneities, C_T are calculated separately, in the first two steps and in the third step, respectively.

In region with tensile hydrostatic stress, hydrogen has a lower chemical potential. Therefore, in order to eliminate the gradient of the chemical potential, the interstitial hydrogen moves from regions with compressive to tensile hydrostatic stress. During the diffusion process, part of the hydrogen is trapped by microstructural defects. However, for simulations at macroscopic level, as the current case, it is not possible to identify each type of traps present into the microstructure and therefore literature relationships that link the trapped hydrogen amount with plastic strain are adopted. Indeed, as shown in Ref. [3], both low and high strength steels present a similar trend for plastic strain and trapped hydrogen amount at a crack tip.

The first step is a static analysis on the as-received material aimed at determining the stress state and in particular the hydrostatic stress field. This is imported into the second step, a mass diffusion analysis that calculates the diffusible hydrogen content. Starting from an initial hydrogen concentration assumed uniform on the entire specimen the analysis computes a redistribution of hydrogen according to the stress state previously calculated. The C_L concentration is finally transferred to the third step, where cohesive elements are introduced to simulate the crack propagation. In the last analysis, a package of user subroutines allows for the calculation of the total hydrogen concentration C and the simulation of the hydrogen effect on the material properties.

In particular, the trapped hydrogen concentration is defined according to the relationship proposed in Ref. [6] based on the data available in Ref. [3].

$$C_T = (49.0 \cdot \epsilon_p + 0.1) \cdot C_L \quad (7)$$

$$C = C_L + C_T$$

The embrittlement induced by hydrogen on the mechanical properties of the material is quantified through a factor k , which depends on the total concentration C as follows [16]:

$$k = \frac{t_0(\theta)}{t_0(0)} = 1 - 1.0467 \cdot \theta + 0.1687 \cdot \theta^2 \quad (8)$$

$$\theta = \frac{C}{C + \exp(\Delta g_b / RT)}$$

where Δg_b is the variation of Gibbs free energy, R is the universal gas constant and T is the absolute temperature. The k factor reduces the cohesive traction stress of the TSL and thus reproduces at macroscopic dimensional level a microstructural HEDE (Hydrogen Enhanced DE-cohesion) mechanism.

It has to be pointed out that in order to ensure a correct transferring of the calculated fields from an analysis to another one, the geometry and the mesh have to be equal over the three steps.

3.1. Implementation – Static analysis

The first static stress analysis employed an elastic-plastic material model. The specimen is loaded under displacement control until the value that corresponds to the maximum experimental load reached before crack propagation initiation.

The hydrostatic stress field has to be written in the result Abaqus file in order to be transferred from the current analysis to the second step. To this end, the following card is inserted in the main file under the **OUTPUT REQUEST** section:

```
*ELFILE, POSITION=AVERAGED AT NODES
SINV
```

For each element the values of the hydrostatic stress, SINV, are extrapolated and averaged at nodes.

3.2. Implementation – Mass diffusion analysis

The Abaqus governing equation of mass diffusion analysis is an extension of Fick's law [17, chapter 6.9], which considers also the diffusion driven by the gradient of the pressure:

$$\mathbf{J} = -sD_L \left[\nabla\phi + k_p \nabla p \right] \quad (9)$$

where ∇ denotes the gradient operator.

Quantity ϕ is the normalized concentration, even known as "activity" of diffusing material. It is defined as the concentration of diffusing material C_L divided by the solubility of the as-received material s . D_L is the diffusivity and k_p is the pressure stress factor, providing diffusion driven by the gradient of the equivalent pressure stress $p = -\frac{1}{3} \text{trace}(\boldsymbol{\sigma}) = -\sigma_h$. The factor k_p is defined as follows:

$$k_p = \frac{\bar{V}_H}{R\Delta T} \phi \quad (10)$$

where R is the universal gas constant and \bar{V}_H is the molar volume fraction of hydrogen in iron. For mass conservation equation is valid:

$$\frac{\partial C}{\partial t} = -\nabla \cdot \mathbf{J} \quad (11)$$

Therefore, substituting eq. 9 into eq. 11, the following expression is obtained [11]:

$$\frac{\partial C_L}{\partial t} = D_L \nabla^2 C_L - D_L \frac{\bar{V}_H}{R\Delta T} (\nabla C_L) \cdot (\nabla \sigma_h) - D_L \frac{\bar{V}_H}{R\Delta T} C_L \nabla^2 \sigma_h \quad (12)$$

For the current step, it is necessary to change the element type definition in DC2D4, which are mass diffusion elements. Furthermore, D_L , s and k_p values need to be added to the definition of the material properties.

If temperature and pressure are assumed constant during the analysis, it is possible to define k_p (linear function of concentration as visible in eq. 10) by assigning two extreme values of k_p and C_L and the intermediate values are linearly interpolated by Abaqus. The initial values of temperature and concentration are assigned into the **PREDEFINED FIELDS** section as follows:

```
*INITIAL CONDITIONS, TYPE=TEMPERATURE
Set_name, T
*INITIAL CONDITIONS, TYPE=CONCENTRATION
Set_name, PHI
```

where the value of T and PHI has to be set by the user. PHI is the normalized concentration ϕ .

The following card, added in the STEP definition, recalls in the current step the stress field previously calculated:

```
*PRESSURE STRESS, FILE=results.filename
```

The result of the analysis is the trend of the normalized hydrogen concentration into the specimen, named in Abaqus as NNC. This can be calculated for each time increment of the analysis or at the last increment, in case of time transient and steady state analyses, respectively.

3.3. Implementation – Cohesive analysis

In the last step, besides the implementation of cohesive elements over the crack propagation plane, the diffusible hydrogen concentration, C_L is imported from the previous step.

```
*INITIAL CONDITIONS, TYPE=FIELD, VARIABLE=1,
FILE=file_name.odb, OUTPUT VARIABLE=NNC
```

The normalized concentration, NNC, is read from the database of the previous analysis and imported as predefined field (FV1).

The calculation of the trapped content, C_T , the total hydrogen concentration C , and the k factor necessary to decrease the cohesive strength are calculated by means of a package including three user subroutines.

The UEXTERNALDB subroutine opens external files needed for other user subroutines at the beginning of the analysis and initializes the value of the user-calculated history information. In particular, the subroutine reads a <job name>.map file that includes a list of continuum and corresponding cohesive elements. Each field, in fact, are computed in the unique Gauss point of the continuum elements and then transferred on the associated cohesive elements. Moreover, the initial value of k is set equal to one for the first increment.

The core of the code is the UVARM subroutine that generates element output. It is called for each increment of the step and through the utility routine GETVRM can access material integration point data. In particular, with respect to the current subroutine GETVRM returns values at the end of the current increment. The subroutine accesses the values of the predefined field FV1, i.e C_L , and the equivalent plastic strain PEEQ that are used into the eqs. 7 and 8. Then, four user-defined output variables, which correspond respectively to C_T , C , θ and k are created. The k value that is referred to the unique integration point of the continuum element is finally saved in a common block to get it transferred from continuum elements to the associated cohesive elements. The k factor is then defined as field variable by means of the USDFLD subroutine and added as **DEPENDENCIES** in the cohesive law definition.

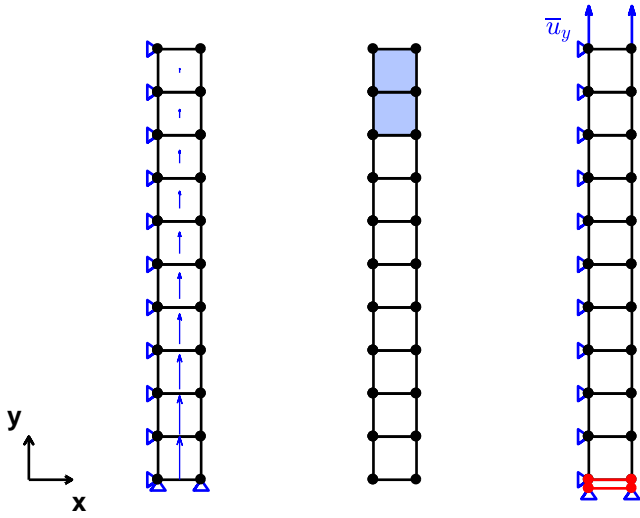


Figure 4: Boundary conditions: step 1 (left), step 2 (center), step 3 (right).

3.4. Example 1: simple strip

Herein, a simple example is reported to illustrate how the code works. It consists of a 2D plane problem, made of a cohesive element and 10 continuum elements vertically placed. Formulation of these elements is the same as the previous example. The analysis runs on three steps in which the following boundary conditions are applied (Fig. 4):

- 1 step: $u_y = 0$ to the two lower nodes of the first continuum element, $u_x = 0$ to all the nodes on the left of the test.
- 2 step: initial hydrogen concentration set uniform on the sample at the beginning of the analysis to simulate the hydrogen charged sample; during the analysis a constant hydrogen flux is applied to the three couples of upper nodes (the two top elements) as environmental hydrogen source.
- 3 step: $u_y = 0$ to the two lower nodes of the cohesive element, $u_x = 0$ to all the nodes on the left of the sample, and the following equations for the node at cohesive and interface nodes:

$$u_{x(1)} = u_{x(3)}, \quad u_{x(2)} = u_{x(4)}, \quad u_{y(3)} = u_{y(4)}$$

where the numeration of the nodes for the cohesive element and the adjacent continuum element is the same as in the first example.

For the current example, in order to obtain a stress gradient in the first step a distributed load gradually increasing with the vertical coordinate is imposed (Fig. 4). It is a gravity load type assigned by means of an analytical field that allows to define a specific value of load for each element (Abaqus card ***DLOAD**). This induces a parabolic stress field and thus a stress gradient. In the second analysis, the mass diffusion, three different

values of initial hydrogen concentration were considered: (i) 1.5 ppm that corresponds to 21.127 NNC, (ii) 1.0 ppm that corresponds to 14.084 NNC and (iii) 0.5 ppm that corresponds to 7.042 NNC. Indeed, in a previous work [15], it was proved that even a quite small hydrogen content, as 0.5 ppm, induces a high embrittling effect with respect to the fatigue and toughness mechanical properties of the tested steel.

The third step implements the cohesive element necessary to simulate the crack propagation process (red element in Fig. 4).

3.5. Results of example 1

Figure 5 reports the main results of the three simulations. The first represents the hydrostatic stress field of the sample obtained by applying the gravity load. The second and the third show the interstitial hydrogen concentration and the k factor values, respectively. Both the results are referred to the case of initial concentration set in mass diffusion analysis equal to 1.5 ppm. The maximum k value is reached in correspondence of the first continuum elements where the plastic strain is higher with respect to the other regions of the sample.

Fig. 6 shows the computed TSL for the three hydrogen concentrations discussed above, along with the baseline TSL for the example presented in sect. 2.1. For increasing initial hydrogen concentration a corresponding reduction of the TSL is shown, according to factor k of eq. (8). It is worth noting that in the present example the damage evolution in the softening range $\delta_1 - \delta_F$ (see Fig. 1) is unstable, because the elastic energy stored in the continuum elements is greater than the energy that can be dissipated by the crack opening. In order to conduct the numerical simulation the ***STATIC, STABILIZE** card is needed: nevertheless only a few points can be computed on the softening part of the TSL. In Fig. 6 the TSL is plotted up to the last valid point, i. e. on the actual TSL and with $\delta < \delta_F$. The next calculated point, due to the finite time step in the numerical integration, already belongs to the failure region ($\delta > \delta_F$ and $\mathfrak{D} = 1$).

3.6. Example 2: C(T) specimen

This last example re-proposes the analysis presented in [18], i. e. the simulations of fracture toughness tests on steel C(T) specimens based on experimental data from [15]. Only half of the specimen is modelled with a simplified geometry, see Fig. 7. The hole at the grips is not included in the model and vertical displacements are applied directly to a vertical strip of nodes in correspondence of the hole axis.

In the present paper a different mesh refinement technique is used with respect to the previous work [18]. The mesh consists in regions of linear quadrilateral elements, and in particular all the elements belonging to the same region have identical size. Passing from outer to inner neighbouring regions, the refinement is abrupt to half the size, and nodes at the boundaries between the regions are connected with linear multi-point constraints (MPC). This technique allows for a structured mesh (within each refinement zone) with equal-sided elements, so that no mesh distortion is introduced. A visual inspection of the results at the transition between two different zones shows limited errors due to the MPC's. On the contrary, other refinement

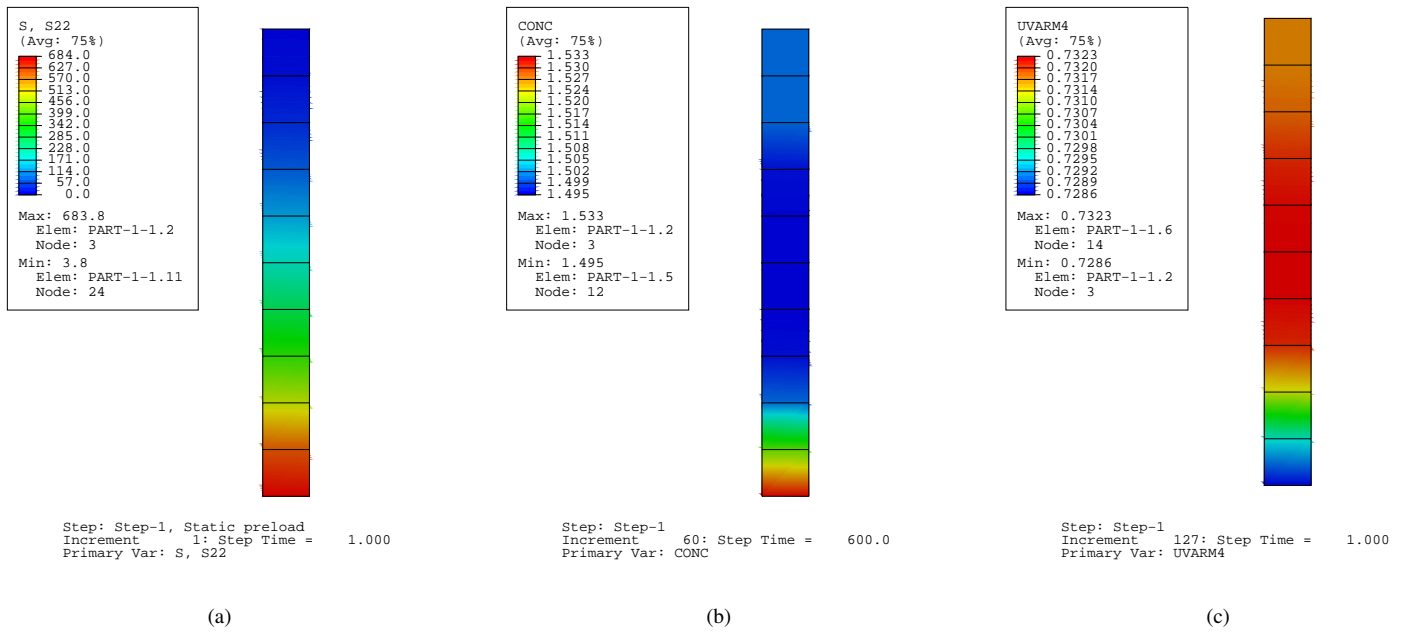


Figure 5: Results of example 1: (a) hydrostatic stress field in MPa, (b) interstitial hydrogen concentration C_L CONC in ppm, (c) k factor trend.

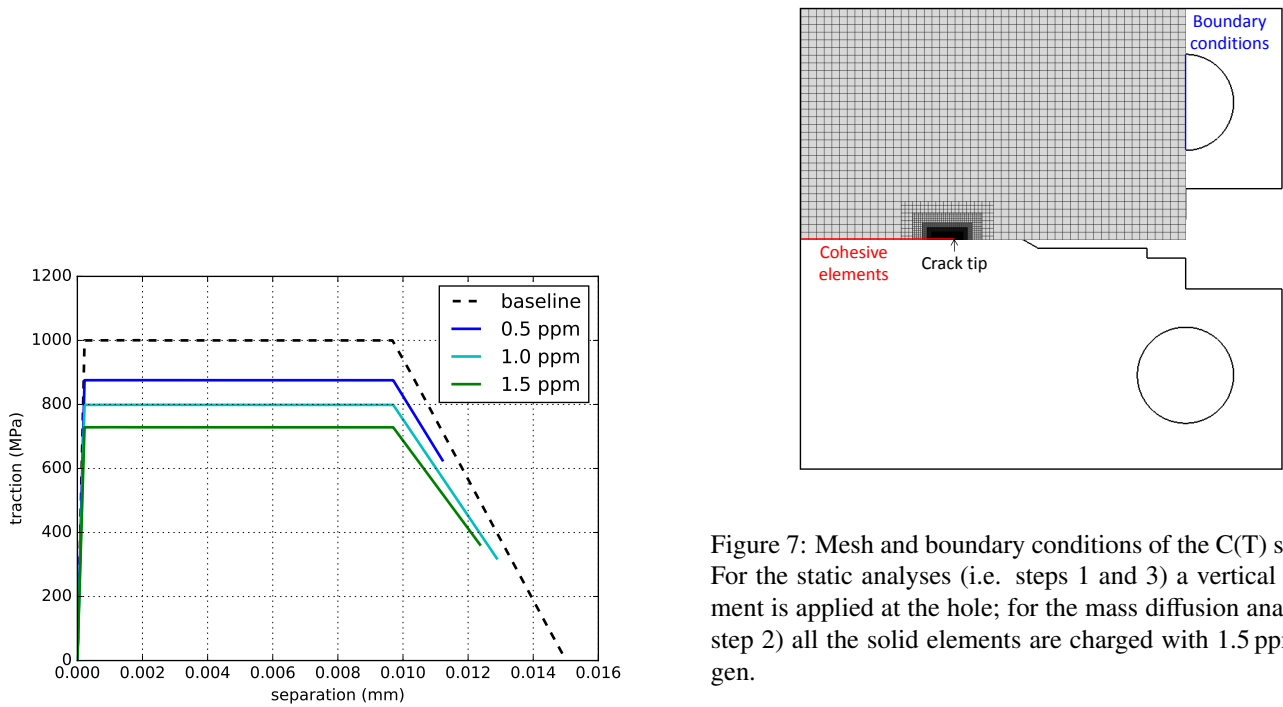


Figure 6: TSL at various initial hydrogen concentrations.

Figure 7: Mesh and boundary conditions of the C(T) specimen. For the static analyses (i.e. steps 1 and 3) a vertical displacement is applied at the hole; for the mass diffusion analysis (i.e. step 2) all the solid elements are charged with 1.5 ppm hydrogen.

techniques introduce mesh distortion, which could result into greater errors, especially in the calculation of the hydrostatic stress gradient and related quantities at the transition regions.

3.7. Results of example 2

At first, a calibration process of the TSL parameters is performed considering the hydrogen uncharged C(T) specimen. Experimental results of crack tip opening displacement and crack

advancement (CTOD vs Δa plots) are used as benchmark for the calibration. The crack length is estimated from the damage state of the cohesive elements at each increment. When $\delta > \delta_F$ and $\mathfrak{D} = 1$, the total crack length moves forward of one element length. Once the calibration of the cohesive properties is concluded, the three-step procedure is applied in order to predict the behaviour of the material containing hydrogen. The results of the three simulations are illustrated in Fig. 8. At the beginning of the mass diffusion analysis, the hydrogen concentration is set to 1.5 ppm in the whole specimen. Further details on the sensitivity of the model to the hydrogen concentration are given in [18], providing the trends of crack tip opening displacement and resulting hydrogen concentration (interstitial and trapped) at the crack tip for a hydrogen concentration between 0.5 and 3 ppm.

The numerical prediction in presence of hydrogen is close to the experimental trend but not fully in agreement. Indeed, the model under-estimates the embrittling effect (see Fig. 9). This can be related to the implementation into the code of the only decohesion mechanism. Other embrittling mechanisms can also be active and interact, such as the local plasticity mechanism [10], but they have not been considered in the implementation.

4. Conclusions

The current paper presents a numerical implementation in a weakly coupled form to simulate hydrogen embrittlement within the commercial FE software Abaqus.

The developed cohesive zone model consists of three steps of simulations that progressively evaluates both the interstitial lattice and the trapped hydrogen contents. The sum of them results in the total hydrogen concentration, the core variable of the study.

Three user subroutines implemented into the model allow for evaluating the hydrogen content in continuum elements, storing the information in a common block, and transferring it to the associated cohesive elements. The hydrogen content is used to decrease the tensile strength of cohesive elements and thus simulate a decohesion mechanism.

The present paper provides a guideline to the comprehension and use of the code which is released under an open source license and is available at [12].

References

- [1] A. Troiano, The role of hydrogen and other interstitials in the mechanical behaviour of metals, Transactions of American Society for Metals ASM 52 (1960) 54–80.
- [2] R. Oriani, The diffusion and trapping of hydrogen in steel, Acta Metallurgica 18 (1) (1970) 147–157. doi:10.1016/0001-6160(70)90078-7.
- [3] A. Taha, P. Sofronis, A micromechanics approach to the study of hydrogen transport and embrittlement, Engineering Fracture Mechanics 68 (6) (2001) 803–837. doi:10.1016/S0013-7944(00)00126-0.
- [4] H. Birnbaum, P. Sofronis, Hydrogen-enhanced localized plasticity-a mechanism for hydrogen-related fracture, Materials Science & Engineering A: Structural Materials: Properties, Microstructure and Processing 176 (1-2) (1994) 191–202. doi:10.1016/0921-5093(94)90975-X.

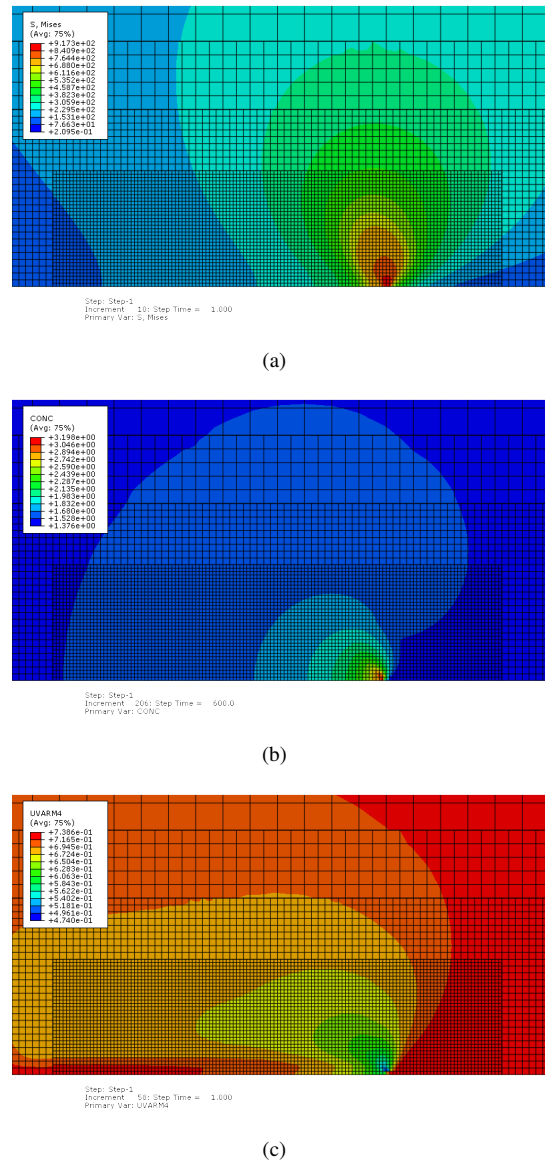


Figure 8: Results of example 2 at the crack tip region: (a) hydrostatic stress field in MPa, (b) interstitial hydrogen concentration C_L CONC in ppm, (c) k factor trend.

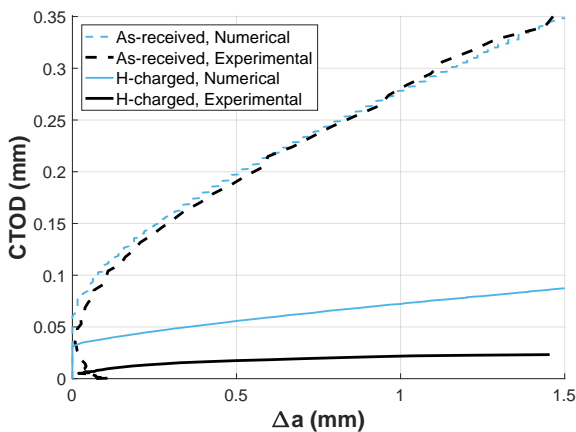


Figure 9: Experimental data from [15] and results of numerical simulations: comparison between as-received and hydrogen charged material.

- [5] J. Lufrano, P. Sofronis, H. Birnbaum, Modeling of hydrogen transport and elastically accommodated hydride formation near a crack tip, *Journal of the Mechanics and Physics of Solids* 44 (2) (1996) 179–205. doi:10.1016/0022-5096(95)00075-5.
- [6] V. Olden, C. Thaulow, R. Johnsen, E. Østby, T. Berstad, Influence of hydrogen from cathodic protection on the fracture susceptibility of 25% Cr duplex stainless steel – Constant load SENT testing and FE-modelling using hydrogen influenced cohesive zone elements, *Engineering Fracture Mechanics* 76 (7) (2009) 827–844. doi:10.1016/j.engfracmech.2008.11.011.
- [7] V. Olden, A. Alvaro, O. M. Akselsen, Hydrogen diffusion and hydrogen influenced critical stress intensity in an API X70 pipeline steel welded joint – Experiments and FE simulations, *International Journal of Hydrogen Energy* 37 (15) (2012) 11474–11486. doi:10.1016/j.ijhydene.2012.05.005.
- [8] A. Alvaro, V. Olden, O. M. Akselsen, 3D cohesive modelling of hydrogen embrittlement in the heat affected zone of an X70 pipeline steel, *International Journal of Hydrogen Energy* 38 (18) (2013) 7539–7549. doi:10.1016/j.ijhydene.2013.02.146.
- [9] A. Alvaro, V. Olden, O. M. Akselsen, 3D cohesive modelling of hydrogen embrittlement in the heat affected zone of an X70 pipeline steel – Part II, *International Journal of Hydrogen Energy* 39 (7) (2014) 3528–3541. doi:10.1016/j.ijhydene.2013.12.097.
- [10] W. Brocks, R. Falkenberg, I. Scheider, Coupling aspects in the simulation of hydrogen-induced stress-corrosion cracking, *Procedia IUTAM* 3 (2012) 11–24. doi:10.1016/j.piutam.2012.03.002.
- [11] C. Moriconi, Modélisation de la propagation de fissure de fatigue assistée par l’hydrogène gazeux dans les matériaux métalliques, Ph.D. thesis, ISAE-ENSMA Ecole Nationale Supérieure de Mécanique et d’Aérotechnique-Poitiers (2012).
URL <https://tel.archives-ouvertes.fr/tel-00784983/>
- [12] The Polihydra project, accessed online Mar 20, 2017.
URL <http://www.polihydra.org>
- [13] K. Park, G. H. Paulino, Computational implementation of the PPR potential-based cohesive model in ABAQUS: educational perspective, *Engineering Fracture Mechanics* 93 (2012) 239–262. doi:10.1016/j.engfracmech.2012.02.007.
- [14] K.-H. Schwalbe, I. Scheider, A. Cornec, Guidelines for applying cohesive models to the damage behaviour of engineering materials and structures, Springer Science + Business Media, 2012. doi:10.1007/978-3-642-29494-5.
- [15] C. Colombo, G. Fumagalli, F. Bolzoni, G. Gobbi, L. Vergani, Fatigue behavior of hydrogen pre-charged low alloy Cr–Mo steel, *International Journal of Fatigue* 83, Part 1 (2016) 2–9, from Microstructure to Design: Advances in Fatigue of Metals. doi:10.1016/j.ijfatigue.2015.

06.002.

- [16] S. A. Serebrinsky, E. A. Carter, M. Ortiz, A quantum-mechanically informed continuum model of hydrogen embrittlement, *Journal of the Mechanics and Physics of Solids* 52 (10) (2004) 2403–2430. doi:10.1016/j.jmps.2004.02.010.
- [17] Dassault Systèmes, Abaqus Analysis User’s Guide (2016).
- [18] G. Gobbi, C. Colombo, L. Vergani, Sensitivity analysis of a 2D cohesive model for hydrogen embrittlement of AISI 4130, *Engineering Fracture Mechanics* 167 (2016) 101–111. doi:10.1016/j.engfracmech.2016.03.045.